HHS Public Access

Author manuscript

*J Tissue Eng Regen Med*. Author manuscript; available in PMC 2018 March 30.

Published in final edited form as:

*J Tissue Eng Regen Med*. 2018 January ; 12(1): e541–e549. doi:10.1002/term.2324.

# Ectopic Models for Endochondral Ossification: Comparing Pellet and Alginate Bead Culture Methods

**Holly E. Weiss-Bilka**[a,1], **Megan E. McGann**[b], **Matthew J. Meagher**[a], **Ryan K. Roeder**[a,b], and **Diane R. Wagner**[c,*]

[a]Bioengineering Graduate Program, University of Notre Dame, Notre Dame, IN 46556, USA

[b]Department of Aerospace and Mechanical Engineering, University of Notre Dame, Notre Dame, IN 46556, USA

[c]Department of Mechanical Engineering, Indiana University-Purdue University Indianapolis, Indianapolis, IN 46202, USA

## Abstract

Key aspects of native endochondral bone development and fracture healing can be mimicked in mesenchymal stem cells (MSCs) through standard *in vitro* chondrogenic induction. Exploiting this phenomenon has recently emerged as an attractive technique to engineer bone tissue, however relatively little is known about the best conditions for doing so. The objective of this study was to compare the bone forming capacity and angiogenic induction of hypertrophic cell constructs containing human adipose-derived stem cells (hASCs) primed for chondrogenesis in two different culture systems: high-density pellets and alginate bead hydrogels. hASC constructs were subjected to 4 weeks of identical chondrogenic induction *in vitro*, encapsulated in an agarose carrier, and then implanted subcutaneously in immune-compromised mice for 8 weeks to evaluate their endochondral potential. At the time of implantation, both pellets and beads expressed aggrecan and type II collagen, as well as alkaline phosphatase (ALP) and type X collagen. Interestingly, ASCs in pellets formed a matrix containing higher glycosaminoglycan and collagen content than that in beads, and ALP activity per cell was higher in pellets. However, after 8 weeks *in vivo*, pellets and beads induced an equivalent volume of mineralized tissue and a comparable level of vascularization. Although osteocalcin and osteopontin-positive osteogenic tissue and new vascular growth was found within both types of constructs, all appeared to be better distributed throughout the hydrogel beads. The results of this ectopic model indicate that hydrogel culture may be an attractive alternative to cell pellets for bone tissue engineering via the endochondral pathway.

### Keywords

endochondral; pellet; alginate bead; adipose-derived stem cells; mineralization; hydrogel encapsulation

*Corresponding author. Address: 723 W. Michigan Ave SL260, Indianapolis, IN, 46220, USA. Tel: 1-317-274-8958; Fax: 1-317-274-9744; wagnerdi@iupui.edu.

[1]Present address: Department of Biological Sciences, 220 Galvin Life Sciences, University of Notre Dame, Notre Dame, IN 46556.

**Conflict of Interest**

The authors declare no conflicts of interest.

## 1. Introduction

Key aspects of the native endochondral bone development process, as well as bone fracture healing through a cartilaginous callus, can be mimicked in mesenchymal stem cells (MSCs) through standard *in vitro* chondrogenic induction. Common features of this process include cartilage matrix formation followed by maturation to a hypertrophic-like phenotype, activation of alkaline phosphatase activity and expression of specific matrix components and growth factors such as type X collagen and vascular endothelial growth factor (VEGF) (Dickhut *et al.*, 2009; Hennig *et al.*, 2007; Iyama, 1991; Pelttari *et al.*, 2006). While up-regulation of such bone and vascular markers is viewed as a shortcoming in efforts to regenerate cartilage, exploiting the natural tendency of these cells to progress through a state resembling hypertrophy has recently emerged as an ideal technique for bone tissue engineering (Thompson *et al.*, 2014). In spite of this, relatively little is known about the optimal conditions for regenerating bone through the endochondral pathway.

The efficacy of utilizing chondrogenic cell constructs to achieve endochondral ossification *in vivo* has been successfully demonstrated with pre-chondrogenic cell line ATDC5 (Weiss *et al.*, 2012), embryonic stem cells (Jukes *et al.*, 2008) and MSCs (Farrell *et al.*, 2011; Pelttari *et al.*, 2006; Scotti *et al.*, 2010; Sheehy *et al.*, 2015). However, despite evidence that adipose-derived stem cells (ASCs) have the ability to form bone through a cartilage intermediate (Yang *et al.*, 2005), a successful *in vivo* model of endochondral ossification has not yet been developed for this particular cell type.

ASCs are an attractive alternative as a therapeutic cell source because they are readily accessible, safe to harvest, and available in larger quantities than bone marrow aspirate (Housman *et al.*, 2002; Lin *et al.*, 2008). They also secrete pro-osteogenic factors such as vascular endothelial growth factor (VEGF), which may enhance bone formation upon implantation (Kondo *et al.*, 2009; Rehman *et al.*, 2004). However, in order to develop an endochondral bone formation model with ASCs, it is first necessary to identify and optimize chondrogenic culture conditions for this specific cell type. Preliminary studies comparing the chondrogenic potential of stem cells derived from adipose tissue and bone marrow reported that ASCs were inferior to their bone marrow-derived stem cell (BMSC) counterparts (Afizah *et al.*, 2007; Huang *et al.*, 2005; Winter *et al.*, 2003). However, it has since been discovered that ASCs are capable of achieving a chondrogenic phenotype comparable to that of BMSCs when treated with an ASC-specific induction medium (Dickhut et al., 2009; Hennig et al., 2007; Kim and Im, 2009).

Biochemical stimulation is only one of two factors critical for successful chondrogenesis *in vitro*. Progenitor cells such as ASCs also require a three-dimensional culture environment to effectively promote chondrogenic differentiation. This has generally been achieved with two culture systems: multicellular aggregates, or cell “pellets” (Danišovic *et al.*, 2007; Dickhut *et al.*, 2009; Estes *et al.*, 2010; Hennig *et al.*, 2007; Kim and Im, 2009), and cell-seeded hydrogels (Erickson *et al.*, 2002; Mehlhorn *et al.*, 2007). The pellet system is attractive in its simplicity, providing an environment rich in cell-cell contacts that is similar to that of mesenchymal cell condensations during embryonic development and native fracture repair. The tightly packed aggregate creates a gradient in oxygen and nutrients from cells on the

outer surface to those at the central core, often reflected in the heterogeneous spatial distribution of chondrogenic pellet tissues (Barry *et al.*, 2001; Dickhut *et al.*, 2009; Pelttari *et al.*, 2006). Cell-seeded hydrogels lack the abundant cell-cell contacts of pellets, but offer several advantages compared to aggregate culture. Porous hydrogels such as alginate confer improved nutrient diffusion and can therefore support larger construct sizes compared to high-density cell pellets (Drury and Mooney, 2003). In addition, cell density and distribution can be tailored to fit the desired application.

Conditions for achieving robust chondrogenesis of ASCs *in vitro* have been developed and optimized over the past decade; however, the response of these cells to different chondrogenic culture modalities such as pellet culture versus hydrogel encapsulation has not been directly compared. Further, the influence of specific culture methods on hypertrophic markers *in vitro* and subsequent endochondral ossification *in vivo* has not been previously investigated. The objective of this study was therefore to directly compare the endochondral response of human ASCs (hASCs) seeded either in pellet culture or in alginate beads. After hASC constructs were primed to a hypertrophic-like state through standard *in vitro* chondrogenic culture, the *in vivo* bone forming capacity and angiogenic induction of hASC pellets and beads was evaluated in an ectopic mouse model.

## 2. Materials and Methods

### 2.1. Cell Culture

Human adipose-derived stem cells (ZenBio, Durham, NC) were expanded as previously described (Estes *et al.*, 2010). All cells in this study were a pooled population from 5 non-diabetic female donors and were derived from subcutaneous adipose tissue. Upon thawing, cells were plated at 8 000 cells/$cm^2$ on T175 tissue culture flasks (Greiner BioOne, Monroe, NC). Subsequent passages were seeded at a density of 3 000 cells/$cm^2$. Cells were maintained in DMEM/F12 medium (1:1) (MediaTech, Herndon, VA) containing 10 % FBS (Atlas Biologicals, Fort Collins, CO), 1 % Pen-Strep (MediaTech), 5 ng/mL hEGF, 1 ng/mL rhFGF and 0.25 ng/mL TGFβ1 (all from PeproTech, Rocky Hill, NJ), Rocky Hill, NJ), which was changed every two days.

For chondrogenic culture, p5 hASCs were collected by centrifugation, counted, and pelleted in 96-well, v-bottom micro-plates or embedded in alginate beads. Pellets were formed by centrifugation of 250 000 cells per well at 300 × g for 5 minutes. Cell-seeded alginate beads were formed based on published methods (Estes *et al.*, 2010). Briefly, collected hASCs were re-suspended in 1.2 % alginate (w/v) (NovaMatrix, Sandvika, Norway) in 150 mM NaCl at 1.5 % (w/v) at a concentration of $8 \times 10^6$ cells/mL. The solution was drawn into a syringe and then dispensed drop-wise with a 22G needle into 102 mM pre-warmed $CaCl_2$ solution in a sterile, agarose-coated 12-well plate. Beads were allowed to polymerize for 5 minutes at 37 °C, after which they were rinsed twice with sterile culture medium (DMEM, 1 % Pen-Strep) for 15 minutes at 37 °C.

Pellets and beads were cultured in a chondrogenic induction medium composed of DMEM-HG (MediaTech), 1 % Pen-Strep supplemented with 1X ITS (Gibco, Life Technologies, Grand Island, NY), 1.25 mg/mL BSA (Fisher Scientific, Pittsburgh, PA), 0.17 mM ascorbic

acid, 0.1 μM dex, 0.35 mM proline (all from Sigma-Aldrich, St. Louis, MO), 1 mM sodium pyruvate (Lonza, Walkersville, MD), and 10 ng/mL BMP6 and 10 ng/mL TGF-β1 (PeproTech), (modified from (Hennig *et al.*, 2007)) for 28 days. Fresh medium was added every other day, and pellets were carefully detached from wells at each medium change.

### 2.2. Biochemical Analysis

DNA was quantified at the time of pellet and bead synthesis (d0) by pipetting 3 drops of cell-containing alginate solution ($n = 3$) or 3 × 250 000-cell aliquots of pellet cell suspension ($n = 3$) directly into centrifuge tubes and processed as described below for d28 samples. For quantification of DNA and sulfated glycosaminoglycan (sGAG) accumulation in d28 *in vitro* samples, 3 pellets or beads were collected per replicate ($n = 3$) and digested in papain solution (125 μg/mL papain, 0.1 M sodium phosphate, 5 mM EDTA, 5 mM L-cysteine, pH 6.5; all products from Sigma-Aldrich) at 60 °C overnight (Estes and Guilak, 2011). Digests were then frozen for future analysis. DNA content of samples was assessed via Quant-iT™ PicoGreen® dsDNA Assay Kit (Invitrogen™, Life Technologies) following manufacturer's instructions. Quantification of sGAG was performed as previously described (Awad *et al.*, 2003; Estes *et al.*, 2010). Briefly, 40 μL of each digested sample was pipetted into wells of a clear, flat-bottom 96-well plate in duplicate. 125 μL of 1,9-dimethylmethylene blue (DMMB) dye was added to each well, mixed, and the optical density (OD) of each well was measured at 540 and 600 nm. The pH of the DMMB dye was adjusted to 1.5 for alginate samples and respective standards to minimize interactions between the dye and carboxyl groups in alginate (Awad *et al.*, 2003; Enobakhare *et al.*, 1996; Estes *et al.*, 2010). Measured OD's for each sample were compared to a chondroitin 4-sulfate standard curve to determine sGAG content, which was then normalized to the sample's DNA content to compensate for differences in cell number between the two groups. For determination of alkaline phosphatase activity (ALP), beads were dissolved in sodium citrate buffer and released cells were collected by centrifugation ($n = 3$). Alternatively, cell pellets were collected and rinsed with sterile PBS. ALP activity was then determined with SensoLyte® pNPP Alkaline Phosphatase Assay Colorimetric Kit (AnaSpec, Fremont, CA), per manufacturer's instructions. The ALP activity of each sample was normalized to its DNA content. Total collagen content of d28 samples ($n = 3$) was assessed via quantification of hydroxyproline by high performance liquid chromatography (HPLC) as previously described (McGann *et al.*, 2012). Briefly, papain-digested samples were lyophilized, hydrolyzed in 6M HCl and then dried. Hydrolysates were dissolved in deionized water with a sarcosine internal standard and subjected to a derivitization process (Hutson *et al.*, 2003). The resulting aqueous phase was used for HPLC. Collagen content was calculated from each hydroxyproline concentration based on an average hydroxyproline fraction of 13 % in human collagens (Ignat'eva *et al.*, 2007). This value was normalized to the average DNA content ($n = 3$) of pellets or beads, as appropriate.

### 2.3. *In Vivo* Study

Samples for implantation were prepared according to Figure 1. Following 28 days of chondrogenic culture, both pellets and beads were embedded in 2 % agarose in PBS to provide a uniform construct size and to aid in retrieval (1 sample per gel; 5 mm diameter × 3 mm height) (Kaps et al., 2002). After overnight incubation, agarose-encapsulated pellet and

cell-seeded alginate bead constructs were either implanted subcutaneously via small incisions in the dorsal region of athymic nude mice (4 constructs per mouse; $n = 6$/group) or harvested for analysis of constructs at the time of implantation ($n = 3$ for biochemical analyses; $n = 3$ for histology). Mice (Harlan Laboratories, Indianapolis, IN) were anesthetized with a 'rodent cocktail' consisting of 100 mg/mL Ketamine, 20 mg/mL Xylazine and 10 mg/mL Acepromazine (all from Butler Schein, Dublin, OH) in sterile saline. Incisions were closed with autoclips, which were removed once the wounds had fully healed. Mice were sacrificed and explants (agarose-encapsulated samples along with surrounding attached tissues) were recovered after 8 weeks *in vivo*. All procedures were approved by the Notre Dame Institutional Animal Care and Use Committee (IACUC) and were performed in compliance with the NIH Guide for Care and Use of Laboratory Animals.

### 2.4. Micro-computed Tomography

Excised samples were fixed in 4 % paraformaldehyde (PFA) in PBS overnight at 4 °C, rinsed thoroughly with PBS and scanned by micro-computed tomography (μCT: μCT-80 Scanco Medical AG, Brüttisellen, Switzerland). Scans were performed at 55 kVp, 145 μA, and 600 ms integration time for 306 or 424 slices with a 0.5 mm Al filter and 10 μm voxel size. The volume of mineralized tissue was quantified by calculating the number of voxels attenuating above a threshold of 212, corresponding to a linear attenuation coefficient of 1.70 $cm^{-1}$ and a hydroxyapatite concentration of 580 $mgHA/cm^3$ as determined by a custom calibration phantom (Deuerling *et al.*, 2010). Following CT scans, samples were decalcified in 0.5 M ethylenediaminetetraacetic acid (EDTA) for 2 weeks prior to histological analysis. Decalcification solution was exchanged every other day.

### 2.5. Histology and Immunohistochemistry

For histological analysis, decalcified samples were fixed, frozen, and cryosectioned (7 μm). To detect alkaline phosphatase activity, sections of 28-day samples were brought to room temperature, hydrated in PBS, and incubated in 1 % magnesium chloride (w/v) in 100 mM Tris-maleate buffer, pH 9.2 solution overnight at room temperature. The following day, sections were incubated in ALP substrate solution (20 mg Naphthol AS-MX phosphate, 40 mg Fast Red TR salt 1,5-naphthalenedisulfonate in 100 mM Tris-maleate buffer, pH 9.2; all from Sigma-Aldrich) at room temperature and mounted in an aqueous medium. To highlight construct morphology before and after implantation, H&E and Masson's Trichrome stains were performed using standard techniques.

All immunofluorescence (IF) procedures were optimized for the specific antibody applied. Unless otherwise noted, IF procedures were performed for aggrecan (goat polyclonal, Santa Cruz Biotechnology, Dallas, TX), type II collagen (rabbit polyclonal; Santa Cruz), type X collagen (rabbit polyclonal, Abcam, Cambridge, MA), osteocalcin (rabbit polyclonal, Abcam), osteopontin (goat polyclonal, R&D Systems, Minneapolis, MN) and CD31 (goat polyclonal, R&D Systems) as follows. Slides were brought to room temperature, hydrated in PBS and subjected to antigen retrieval in 1 mM EDTA, 0.05 %(v/v) Polysorbate −20, pH 8.0 at 90 °C for 5 minutes. Sections were then cooled to room temperature, rinsed in PBS and marked with a PAP pen. Blocking was performed in PBS containing 0.3 M glycine and 1 – 3 % (v/v) normal serum of the animal in which the secondary antibody was raised. Primary

antibodies were applied overnight at 4 °C, after which sections were rinsed with PBS. Fluorescent secondary antibodies (Alexa Fluor® anti-goat IgG and anti-rabbit IgG, Invitrogen™) were applied for 1 hour. Finally, sections were rinsed in distilled water and mounted in an aqueous medium containing 4′,6-Diamidino-2-Phenylindole (DAPI; Vector Labs, Burlingame, CA). Heat-mediated antigen retrieval was omitted for osteopontin.

For human nuclei antibody, sections were brought to room temperature, permeabilized with ice cold acetone for 10 minutes at room temperature, dried and re-hydrated in PBS. Blocking was performed in two steps: first with 3 % (v/v) normal donkey serum and 0.3 M glycine in PBS for 30 minutes, and then with Mouse IgG Blocking Reagent (Vector Labs). Primary antibody was applied (mouse monoclonal 235-1 IgG1, Rockland, Gilbertsville, PA) for 1 hour, sections were rinsed with PBS, and the secondary antibody (Alexa Fluor® anti-mouse, Invitrogen™) was applied for 20 minutes. All nuclei were counterstained with DAPI (Vector Labs), and endogenous fluorescence was quenched for 1 minute with Trypan blue (250 μg/mL, pH 4.4, Invitrogen™) (Mosiman *et al.*, 1997).

### 2.6. Quantification and Statistical Analysis

Blood vessel infiltration into the constructs was determined by quantifying the number of CD31+ vessels using a custom MATLAB (MathWorks, Natick, MA) program (100× magnification, $n = 6$), while the cellularity of the constructs was reported as the number of DAPI-positive cells per cross-section. A measure of vascular density was obtained by normalizing the number of blood vessels to the total number of cells. The presence of red blood cell-containing lumina was verified via high magnification bright field microscopy and H&E staining (Figure S1). Statistical analyses were performed in Prism (GraphPad, La Jolla, CA). Significance was assessed by Student's t-test or 2-way ANOVA and Tukey's post-hoc test ($p < 0.05$). Data are presented as mean ± SEM.

## 3. Results

### 3.1. *In vitro* analysis

**3.1.1. DNA and biochemical quantification—**Histological evaluation of samples at the time of implantation highlighted the size differential between the two culture types, as the diameter of the beads was approximately twice that of the pellets (Figure 2A,B). Further inspection of H&E stained sections confirmed the presence of enlarged cells, characteristic of hypertrophic chondrocytes, in both cell pellets and cell-seeded alginate beads (Figure 2A,B insets). Quantification of DNA content in hASC pellets and alginate beads at day 0 confirmed that each group began with a comparable number of cells (Figure 2C). However, following 28 days of culture in a chondrogenic induction medium, the DNA content of pellets decreased by 60 % compared to day 0 (1291.80 ± 59.38 vs. 519.01 ± 18.16 ng DNA). Conversely, the DNA content of alginate beads remained unchanged. At both time points, beads contained significantly more DNA than day 28 pellets. Quantitative assessment of chondrogenic markers in day 28 constructs (Figure 2D,E) revealed that there was significantly higher collagen content (pellets: 0.0480 ± 0.0029; beads: 0.0078 ± 0.0008 μg collagen/ng DNA) and sGAG content, relative to DNA, in pellets than in beads (9.11 ± 1.26 vs. 0.86 ± 0.22 μg sGAG/ng DNA). The total level of hypertrophic marker ALP was

comparable in pellets and beads (Figure 2F), but interestingly the average ALP per cell in pellets was higher than that measured in beads (0.03846 ± 0.00068 vs. 0.0076 ± 0.0028 ng ALP/ng DNA; Figure 2G).

#### 3.1.2. Distribution of chondrogenic and hypertrophic markers—

Immunohistochemistry confirmed the quantitative biochemical analyses and revealed the spatial distribution of chondrogenic markers type II collagen (Col II) and aggrecan (AGC; Figure 3A,B,E,F). Both markers were well distributed and in discrete locations throughout alginate beads, while AGC staining was more diffuse and Col II appeared to be concentrated in a ring at the periphery of pellets. Analysis of type X collagen (Col X) and ALP activity established that hypertrophic markers were present in both pellets and alginate beads (Figure 3C,D,G,H). ALP staining resembled that of Col II for pellets and beads; staining was primarily located on the periphery of pellets (Figure 3C), while beads contained localized areas of staining throughout the cross-sectional area (Figure 3G). Col X appeared to be stronger and more abundant than Col II in each respective culture system and followed a pattern similar to that of AGC, as staining was more diffuse in pellets (Figure 3D) and was localized to isolated pockets in beads (Figure 3H).

### 3.2. *In vivo* study

**3.2.1. Osteogenesis—**After 8 weeks implantation at an ectopic site, histological analysis revealed cell pellets appeared to remain fully intact (Figure 4A,B), while appreciable degradation was seen within alginate beads (Figure 4E,F). Masson's Trichrome staining indicated that the pellet matrix was largely comprised of collagen (Figure 4B), while there was less collagen matrix in beads (Figure 4E). Both pellets and beads contained osteocalcin- (OCN) and osteopontin- (OPN) positive tissue, though the distribution of these markers differed according to construct type. In pellets, OCN and OPN were localized to regions at the periphery of the cellular condensation (Figure 4C,D), whereas in beads the markers were diffuse throughout the entire alginate matrix (Figure 4G,H). There was no evidence of residual cartilaginous tissue within pellets or beads as assessed by histological evaluation of Col II and AGC staining (data not shown). Inspection of tissues by μCT confirmed that constructs contained mineralized deposits primarily on the exterior of the encapsulating agarose hydrogel (Figure 4I, insets). Quantitative analysis demonstrated substantial variation in the amount of mineralization induced by both pellet- and bead-containing constructs (Figure 4I), and there was no significant difference in the average volume of mineralized tissue in pellet constructs compared to beads.

**3.2.2. Vascularization—**Immunofluorescent staining with CD31 and H&E staining demonstrated that blood vessels had infiltrated all constructs (Figure 5A,B and Supplemental Figure 1). As with osteogenic markers, vascular invasion appeared to be predominantly localized to the peripheral region of pellets, while vessels were evident throughout the entire cross-sectional area of beads. There tended to be a higher degree of vascularization (110.0 ± 37.15 vs. 30.17 ± 10.01 blood vessels per section; Figure 5C) and more cells overall (416.0 ± 76.31 vs. 216.7 ± 48.74; Figure 5D) in beads than in pellets. The vessel density relative to cell number was comparable between groups (Figure 5E).

**3.2.3. Presence and location of implanted hASCs—**The presence of implanted hASCs was assessed by identifying cells positive for human nuclear antigen (HNA). Human cells were thus distinguished from DAPI-positive murine cells by dual HNA and DAPI staining. Qualitative assessment indicated that the hASCs persisted in pellets more than in alginate beads. In pellets, many cells of human origin persisted at both the center and periphery of the cellular condensation (Figure 6A). However, few human cells were detected in beads, and those that remained were located at the center of the residual alginate matrix (Figure 6B).

## 4. Discussion

Thus far, strategies for engineering replacement bone tissue have typically focused on direct bone formation through the intramembranous pathway. However, recent studies have begun to investigate bone regeneration via a cartilage intermediate (Farrell *et al.*, 2011; Jukes *et al.*, 2008; Pelttari *et al.*, 2006; Scotti *et al.*, 2010; Scotti *et al.*, 2013; Weiss *et al.*, 2012). This method aims to mimic the endochondral pathway as it relates to initial long bone development and native fracture healing (Lenas *et al.*, 2009a; Lenas *et al.*, 2009b). Here we demonstrate the capacity of hASCs to induce ectopic mineralization, as well as osteogenesis and vascularization within chondrogenic implants.

Following 4 weeks of identical chondrogenic induction *in vitro*, both hASC pellets and hASC-seeded alginate beads had developed a cartilage-like matrix expressing chondrogenic markers Col II and AGC as well as hypertrophic markers Col X and ALP. All four markers were concentrated in small, discrete regions throughout alginate beads, consistent with the findings of other groups (Erickson *et al.*, 2002; Estes *et al.*, 2006; Estes *et al.*, 2010; Mehlhorn *et al.*, 2007). In pellets, however, chondrogenic and hypertrophic markers followed one of two patterns after 4 weeks of culture; AGC and Col X staining was found primarily in the central regions of pellets, while Col II and ALP staining was located in the band of dense tissue at the pellet periphery. These patterns are also similar to those reported by others (Dickhut *et al.*, 2009; Hennig *et al.*, 2007).

Biochemical analysis of constructs highlighted significant differences in the composition of the chondrogenic tissues. Following 28 days of culture, pellets contained significantly higher quantities of collagen, sGAG and ALP activity per cell than alginate beads, and more collagen and sGAG overall. Pellets lost approximately 60 % of their DNA content over the culture period, though there was no evidence of necrosis in the central region of the aggregate. The progressive loss of cells throughout pellet culture is commonly observed (Sekiya *et al.*, 2002), and may be related to inadequate nutrient diffusion (Vidal *et al.*, 2008). Interestingly, the DNA content of alginate beads did not change significantly over the course of 4 weeks in culture, and was significantly higher than that of the cell pellets at the time of implantation. Taken together, these results appeared to indicate that pellet culture was superior to alginate hydrogel encapsulation with respect to *in vitro* chondrogenic induction of hASCs. Furthermore, based on ALP activity and Col X staining, ASCs in pellets seemed to display a more hypertrophic phenotype.

For *in vivo* implantation, both pellets and beads were encapsulated within an agarose carrier to control for overall construct size and to facilitate sample recovery. Agarose encapsulation would have been particularly important in locating and analyzing the implants in the event that either of the construct types had failed to induce mineralization, as both pellets (Dickhut *et al.*, 2009) and alginate (Yang *et al.*, 2009) can degrade upon *in vivo* implantation, rendering them irretrievable. The hydrogel carrier may have delayed direct communication between the host and implanted cells and increased the diffusion distance for paracrine molecules, resulting in mineral deposits primarily at the periphery of the constructs rather than at their center. However, histological analysis revealed the presence of channels running through the agarose surrounding both pellets and beads, indicating that communication between host and implant was established over time.

Despite differences in the extent of chondrogenesis *in vitro*, the average mineral volume induced by beads and pellets *in vivo* was equivalent, indicating that chondrogenic matrix markers at the time of implantation may not accurately reflect the endochondral response *in vivo*. ALP quantified from constructs at the time of implantation, however, was representative of the mineralization response, as has been previously suggested (Dickhut *et al.*, 2009). Mineralized tissue was largely located at the exterior surface of constructs, consistent with the findings of previous ectopic studies with MSC-seeded hydrogels (Farrell *et al.*, 2011; Scotti *et al.*, 2013; Shimono *et al.*, 2011) and MSC pellets (Farrell *et al.*, 2011; Scotti *et al.*, 2010). This type of peripheral response at the interface of host and implanted tissues suggests that interactions between host and donor cells may be active in the endochondral regenerative strategy.

While there was no frank bone formation within implanted constructs, osteocalcin and osteopontin-positive matrix demonstrated an osteogenic response in both pellets and beads. In pellets, these markers appeared to accumulate preferentially in the area adjacent to channels through which the host tissue had infiltrated the agarose hydrogel, whereas osteocalcin and osteopontin staining was diffuse throughout the remaining alginate matrix in beads. A similar trend was observed with respect to the distribution of blood vessels, which were generally located only at the periphery of pellets, but were found throughout the entire cross-section of beads. These differences may be due to the fact that alginate beads had undergone noticeable dissolution by 8 weeks, while pellets remained fully intact. Moreover, beads tended to have more blood vessels and cells, but not a higher vessel density, suggesting that the differences in vascularity and cellularity may be related. The breakdown of alginate matrix *in vivo* may have allowed for improved neovascularization and nutrient availability in beads (Sheehy *et al.*, 2015), leading to wider distribution of osteogenic markers and vascular invasion in these constructs. This hypothesis was supported by the infiltration of host cells in 8-week constructs.

Implanted hASCs were abundant in explanted pellets, while there were few, if any, human cells detected in beads. Those that remained were located toward the center of the residual alginate matrix. In both cases, hASCs were not observed in the tissue surrounding the agarose carrier or in the blood vessels present within the constructs. A previous study reported a host-dominated endochondral response for collagen-GAG scaffolds containing human MSCs (Farrell *et al.*, 2011), in which osteoblasts lining *de novo* bone tissue were

predominantly of host origin. This is in contrast to ectopic studies in which hASCs partially contributed to neovascularization (Scherberich *et al.*, 2007; Müller *et al.*, 2010) and *de novo* bone formation (Hicok *et al.*, 2004). However, these studies differed from the current one in that the hASCs were either maintained in growth medium, implanted within hours of harvest from donor tissue, or were differentiated to the osteogenic lineage. The extent of hASC contribution to the osteogenic response is unclear, as the mineralized tissue was similar between pellets and beads, while the number of human cells present after 8 weeks *in vivo* differed greatly.

Together, these findings suggest that hASCs are capable of inducing a mineralization response from both high-density cell pellet and cell-encapsulated alginate bead culture methods, perhaps via interactions with host cells. *In vitro*, pellets appeared to induce a more mature chondrogenic phenotype in hASCs than did alginate beads. However, the comparable levels of mineralization and vascularization in each system, along with better cell retention *in vitro* and improved distribution of osteogenic and vascular markers *in vivo* indicate that alginate beads may be a promising method for bone tissue engineering via the endochondral pathway. Furthermore, because nutrient diffusion is improved in alginate beads compared to cell pellets, larger implant sizes may be more feasible. Thus, hydrogel culture may be a more relevant means of translating these experimental methods to clinical applications in the future.

## Supplementary Material

Refer to Web version on PubMed Central for supplementary material.

## Acknowledgments

The authors would like to thank the staff at the University of Notre Dame Freimann Life Sciences Center, the Center for Environmental Science and Technology (CEST), and Dr. Travis Turnbull for his assistance with μCT. The research was supported by the US Army Medical Research & Materiel Command W81XWH-0901-0741. This publication was made possible in part by Grant TL1TR001107 (A. Shekhar, PI) from the National Institutes of Health, National Center for Advancing Translational Sciences, Clinical and Translational Sciences Award.

## References

Afizah H, Yang Z, Hui JHP, et al. A comparison between the chondrogenic potential of human bone marrow stem cells (BMSCs) and adipose-derived stem cells (ADSCs) taken from the same donors. Tissue Eng. 2007; 13:659–66. [PubMed: 17371203]

Awad HA, Halvorsen YC, Gimble JM, et al. Effects of transforming growth factor beta1 and dexamethasone on the growth and chondrogenic differentiation of adipose-derived stromal cells. Tissue Eng. 2003; 9:1301–12. [PubMed: 14670117]

Barry F, Boynton RE, Liu B, et al. Chondrogenic differentiation of mesenchymal stem cells from bone marrow: differentiation-dependent gene expression of matrix components. Exp Cell Res. 2001; 268:189–200. [PubMed: 11478845]

Danišovic L, Lesný P, Havlas V, et al. Chondrogenic differentiation of human bone marrow and adipose tissue-derived mesenchymal stem cells. J Appl Biomed. 2007; 5:139–50.

Deuerling JM, Rudy DJ, Niebur GL, et al. Improved accuracy of cortical bone mineralization measured by polychromatic microcomputed tomography using a novel high mineral density composite calibration phantom. Med Phys. 2010; 37:5138–45. [PubMed: 20964233]

Dickhut A, Pelttari K, Janicki P, et al. Calcification or dedifferentiation: requirement to lock mesenchymal stem cells in a desired differentiation stage. J Cell Physiol. 2009; 219:219–26. [PubMed: 19107842]

Drury JL, Mooney DJ. Hydrogels for tissue engineering: scaffold design variables and applications. Biomaterials. 2003; 24:4337–51. [PubMed: 12922147]

Enobakhare BO, Bader DL, Lee DA. Quantification of sulfated glycosaminoglycans in chondrocyte/alginate cultures, by use of 1,9-dimethylmethylene blue. Anal Biochem. 1996; 243:189–91. [PubMed: 8954546]

Erickson GR, Gimble JM, Franklin DM, et al. Chondrogenic potential of adipose tissue-derived stromal cells in vitro and in vivo. Biochem Biophys Res Commun. 2002; 290:763–9. [PubMed: 11785965]

Estes BT, Guilak F. Three-dimensional culture systems to induce chondrogenesis of adipose-derived stem cells. Methods Mol Biol. 2011; 702:201–17. [PubMed: 21082404]

Estes BT, Diekman BO, Gimble JM, et al. Isolation of adipose-derived stem cells and their induction to a chondrogenic phenotype. Nat Protoc. 2010; 5:1294–311. [PubMed: 20595958]

Estes BT, Wu AW, Guilak F. Potent induction of chondrocytic differentiation of human adipose-derived adult stem cells by bone morphogenetic protein 6. Arthritis Rheum. 2006; 54:1222–32. [PubMed: 16572454]

Farrell E, Both SK, Odörfer KI, et al. In-vivo generation of bone via endochondral ossification by in-vitro chondrogenic priming of adult human and rat mesenchymal stem cells. BMC Musculoskelet Disord. 2011; 12:31–9. [PubMed: 21281488]

Hennig T, Lorenz H, Thiel A, et al. Reduced chondrogenic potential of adipose tissue derived stromal cells correlates with an altered TGFbeta receptor and BMP profile and is overcome by BMP-6. J Cell Physiol. 2007; 211:682–91. [PubMed: 17238135]

Hicok KC, Du Laney TV, Zhou YS, et al. Human adipose-derived adult stem cells produce osteoid in vivo. Tissue Eng. 2004; 10:371–80. [PubMed: 15165454]

Housman TS, Lawrence N, Mellen BG, et al. The safety of liposuction: results of a national survey. Dermatol Surg. 2002; 28:971–8.

Huang JI, Kazmi N, Durbhakula MM, et al. Chondrogenic potential of progenitor cells derived from human bone marrow and adipose tissue: a patient-matched comparison. J Orthop Res. 2005; 23:1383–9. [PubMed: 15936917]

Hutson PR, Crawford ME, Sorkness RL. Liquid chromatographic determination of hydroxyproline in tissue samples. J Chromatogr B Analyt Technol Biomed Life Sci. 2003; 791:427–30.

Ignat'eva NY, Danilov N, Averkiev S, et al. Determination of hydroxyproline in tissues and the evaluation of the collagen content of the tissues. J Anal Chem. 2007; 62:51–7.

Iyama KI. Spatiotemporal pattern of type X collagen gene expression and collagen deposition in embryonic chick vertebrae undergoing endochondral ossification. Anat Rec. 1991; 229:462. [PubMed: 2048750]

Jukes JM, Both SK, Leusink A, et al. Endochondral bone tissue engineering using embryonic stem cells. Proc Natl Acad Sci U S A. 2008; 105:6840–5. [PubMed: 18467492]

Kaps C, Bramlage C, Smolian H, et al. Bone morphogenetic proteins promote cartilage differentiation and protect engineered artificial cartilage from fibroblast invasion and destruction. Arthritis Rheum. 2002; 46:149–62. [PubMed: 11817587]

Kim H, Im G. Combination of transforming growth factor-beta2 and bone morphogenetic protein 7 enhances chondrogenesis from adipose tissue-derived mesenchymal stem cells. Tissue Eng Part A. 2009; 15:1543–51. [PubMed: 19072523]

Kondo K, Shintani S, Shibata R, et al. Implantation of adipose-derived regenerative cells enhances ischemia-induced angiogenesis. Arterioscler Thromb Vasc Biol. 2009; 29:61–6. [PubMed: 18974384]

Lenas P, Moos M, Luyten FP. Developmental engineering: a new paradigm for the design and manufacturing of cell-based products. Part I: from three-dimensional cell growth to biomimetics of in vivo development. Tissue Eng Part B Rev. 2009a; 15:381–94. [PubMed: 19505199]

Lenas P, Moos M, Luyten FP. Developmental engineering: a new paradigm for the design and manufacturing of cell-based products. Part II: from genes to networks: tissue engineering from the

viewpoint of systems biology and network science. Tissue Eng Part B Rev. 2009b; 15:395–422. [PubMed: 19589040]

Lin K, Matsubara Y, Masuda Y, et al. Characterization of adipose tissue-derived cells isolated with the Celution system. Cytotherapy. 2008; 10:417–26. [PubMed: 18574774]

McGann ME, Vahdati A, Wagner DR. Methods to assess in vitro wear of articular cartilage. Proc Inst Mech Eng H. 2012; 226:612–22. [PubMed: 23057234]

Mehlhorn AT, Niemeyer P, Kaschte K, et al. Differential effects of BMP-2 and TGF-beta1 on chondrogenic differentiation of adipose derived stem cells. Cell Prolif. 2007; 40:809–23. [PubMed: 18021172]

Mosiman VL, Patterson BK, Canterero L, et al. Reducing cellular autofluorescence in flow cytometry: an in situ method. Cytometry. 1997; 30:151–6. [PubMed: 9222101]

Müller A, Mehrkens A, Schäfer D, et al. Towards an intraoperative engineering of osteogenic and vasculogenic grafts from the stromal vascular fraction of human adipose tissue. Eur Cell Mater. 2010; 19:127–35. [PubMed: 20198567]

Pelttari K, Winter A, Steck E, et al. Premature induction of hypertrophy during in vitro chondrogenesis of human mesenchymal stem cells correlates with calcification and vascular invasion after ectopic transplantation in SCID mice. Arthritis Rheum. 2006; 54:3254–66. [PubMed: 17009260]

Rehman J, Traktuev D, Li J, et al. Secretion of angiogenic and antiapoptotic factors by human adipose stromal cells. Circulation. 2004; 109:1292–8. [PubMed: 14993122]

Scherberich A, Galli R, Jaquiery C, et al. Three-dimensional perfusion culture of human adipose tissue-derived endothelial and osteoblastic progenitors generates osteogenic constructs with intrinsic vascularization capacity. Stem Cells. 2007; 25:1823–9. [PubMed: 17446558]

Scotti C, Piccinini E, Takizawa H, et al. Engineering of a functional bone organ through endochondral ossification. Proc Natl Acad Sci U S A. 2013; 110:3997–4002. [PubMed: 23401508]

Scotti C, Wirz D, Wolf F, et al. Engineering human cell-based, functionally integrated osteochondral grafts by biological bonding of engineered cartilage tissues to bony scaffolds. Biomaterials. 2010; 31:2252–9. [PubMed: 20022102]

Sekiya I, Vuoristo JT, Larson BL, et al. In vitro cartilage formation by human adult stem cells from bone marrow stroma defines the sequence of cellular and molecular events during chondrogenesis. Proc Natl Acad Sci U S A. 2002; 99:4397–402. [PubMed: 11917104]

Sheehy EJ, Mesallati T, Vinardell T, et al. Engineering cartilage or endochondral bone: a comparison of different naturally derived hydrogels. Acta Biomater. 2015; 13:245–53. [PubMed: 25463500]

Shimono K, Tung W, Macolino C, et al. Potent inhibition of heterotopic ossification by nuclear retinoic acid receptor-γ agonists. Nat Med. 2011; 17:454–60. [PubMed: 21460849]

Thompson EM, Matsiko A, Farrell E, et al. Recapitulating endochondral ossification: a promising route to in vivo bone regeneration. J Tissue Eng Regen Med. 2014; 9:889–902. [PubMed: 24916192]

Vidal MA, Robinson SO, Lopez MJ, et al. Comparison of chondrogenic potential in equine mesenchymal stromal cells derived from adipose tissue and bone marrow. Vet Surg. 2008; 37:713–24. [PubMed: 19121166]

Weiss HE, Roberts SJ, Schrooten J, et al. A semi-autonomous model of endochondral ossification for developmental tissue engineering. Tissue Eng Part A. 2012; 18:1334–43. [PubMed: 22394057]

Winter A, Breit S, Parsch D, et al. Cartilage-like gene expression in differentiated human stem cell spheroids: a comparison of bone marrow-derived and adipose tissue-derived stromal cells. Arthritis Rheum. 2003; 48:418–29. [PubMed: 12571852]

Yang C, Frei H, Rossi FM, et al. The differential in vitro and in vivo responses of bone marrow stromal cells on novel porous gelatin–alginate scaffolds. J Tissue Eng Regen Med. 2009; 3:601–14. [PubMed: 19685485]

Yang M, Ma QJ, Dang GT, et al. In vitro and in vivo induction of bone formation based on ex vivo gene therapy using rat adipose-derived adult stem cells expressing BMP-7. Cytotherapy. 2005; 7:273–81. [PubMed: 16081354]

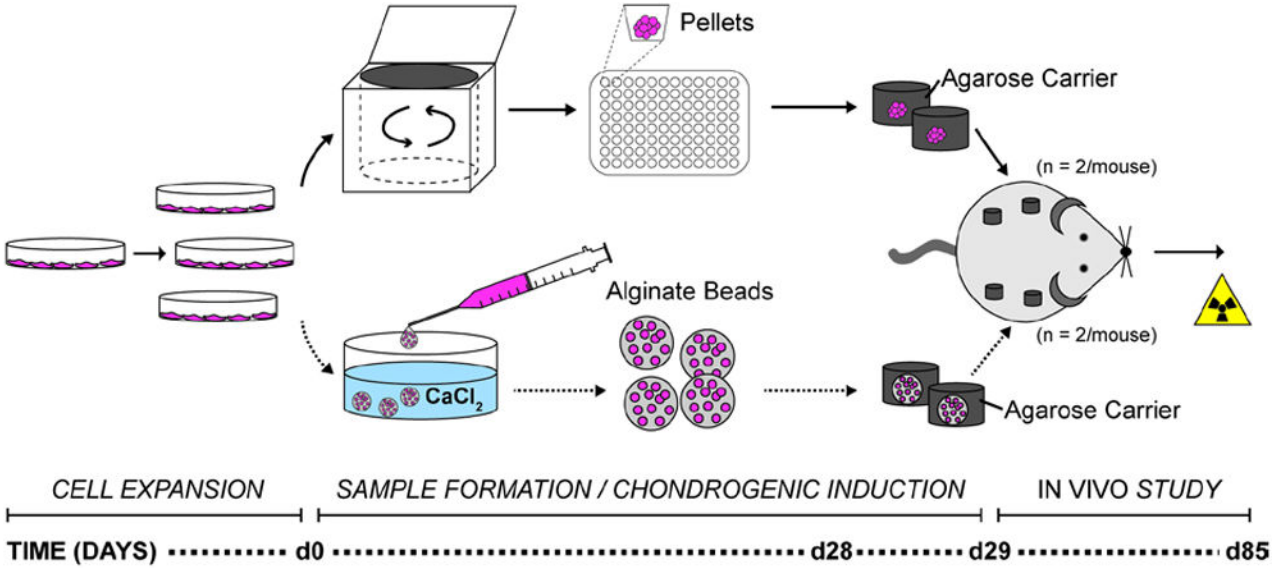


**Figure 1.**

Experimental overview. hASCs were expanded in monolayer *in vitro* and then collected for cell pellet formation via centrifugation or alginate bead formation. Samples were cultured in chondrogenic induction medium for 4 weeks, encapsulated in agarose carriers and maintained overnight in chondrogenic medium prior to subcutaneous implantation in the cervical region of immune-compromised mice. After 8 weeks *in vivo*, samples were removed, scanned by μCT and processed for histological evaluation.

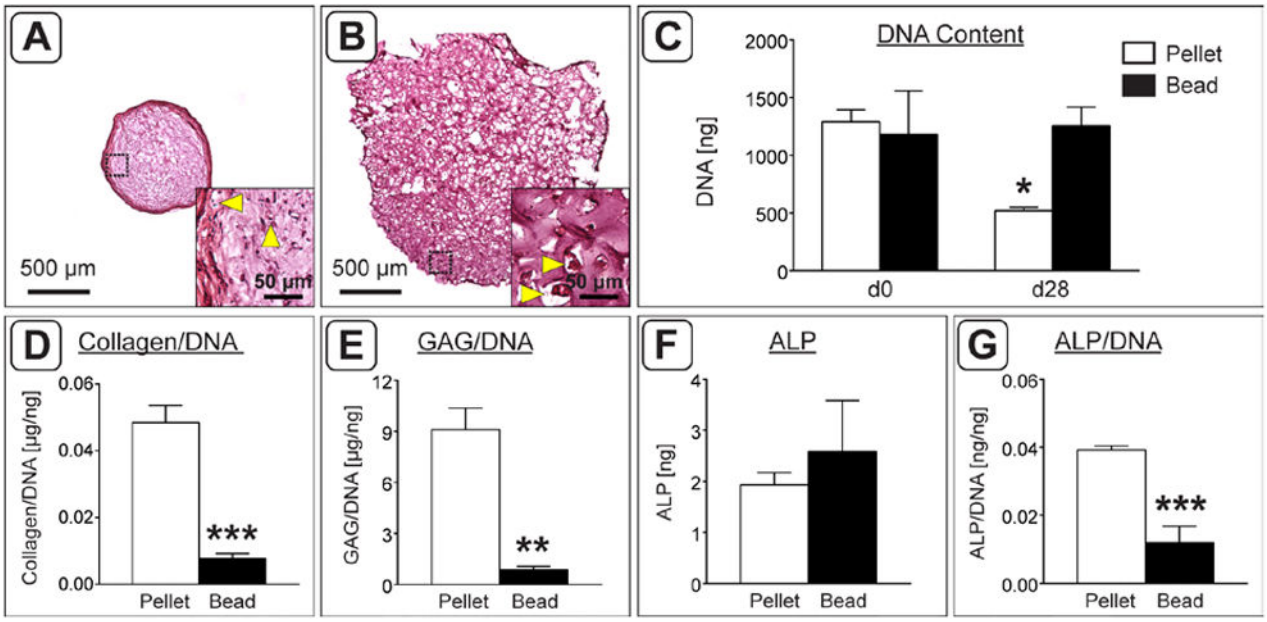


**Figure 2.**

Implant size and biochemical analysis at the time of implantation. A,B) H&E staining of pellet (A) and alginate bead (B) constructs following 4 weeks of chondrogenic induction *in vitro*. Black dashed boxes indicate the region magnified in insets. Yellow arrowheads indicate the presence of enlarged cells with a hypertrophic morphology. C) Starting DNA content (d0) compared to DNA content after 4 weeks in culture (d28). Pellets at 28 days contained significantly fewer cells than all other groups. D) Total collagen content normalized to the average DNA content. E) sGAG content of each construct normalized to its DNA content. F,G) Total ALP activity (F) and ALP activity normalized to DNA content (G). ($n = 3$; *: $p < 0.05$, **: $p < 0.01$, ***: $p < 0.001$, ****: $p < 0.0001$).

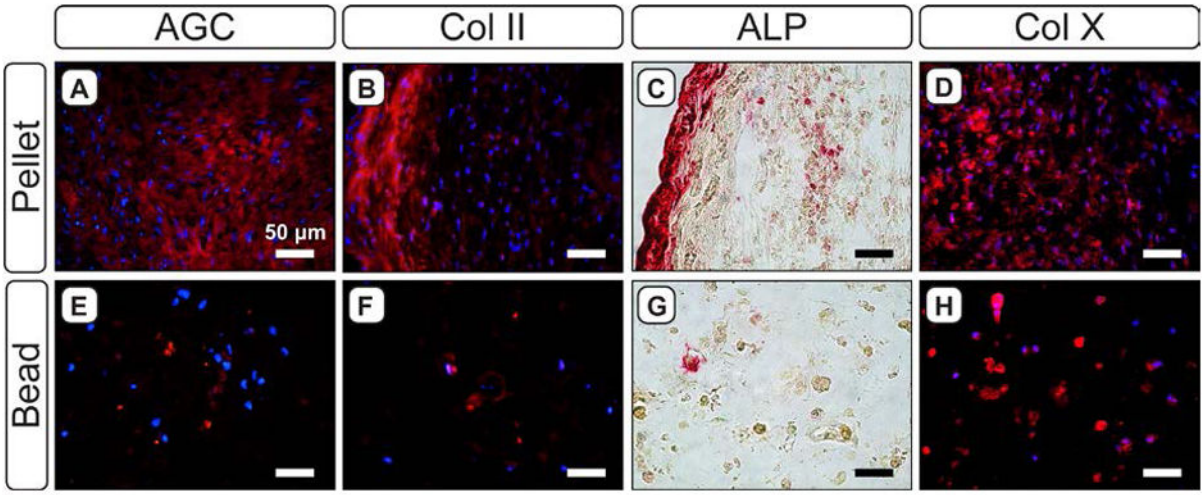


**Figure 3.**

Evaluation of chondrogenic and hypertrophic markers in 4-week pellets (A–D) and alginate beads (E–H). For aggrecan (AGC; A,E), type II collagen (Col II; B,F) and type X collagen (Col X; D,H), red staining indicates the marker of interest; blue staining indicates cell nuclei (DAPI). C,G) Red staining indicates the presence of ALP activity.

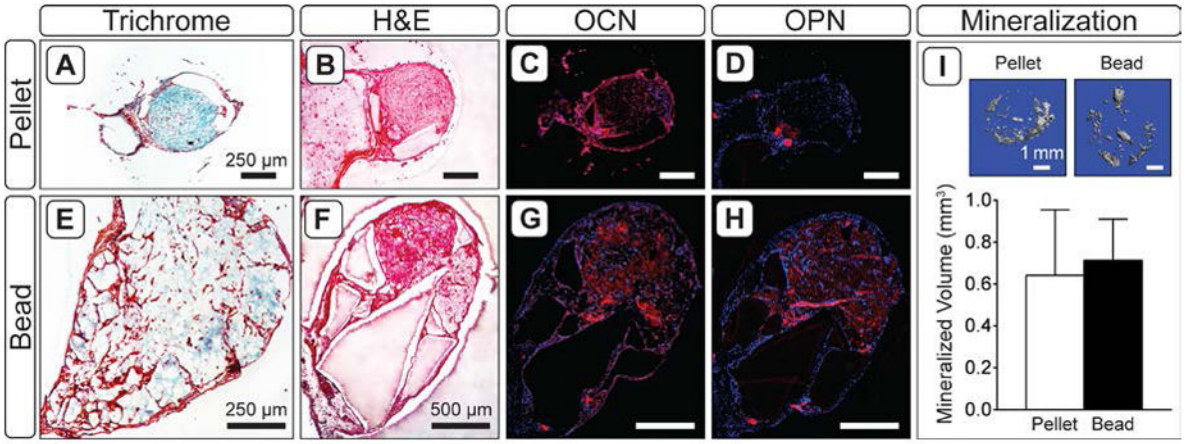


**Figure 4.**

Tissue morphology by Masson's Trichrome (A,E) and H&E (B,F), and osteogenic markers (C,G; D,H) in 8 week explants. For osteocalcin (C,G) and osteopontin (D,H), red staining indicates the marker of interest; blue staining indicates cell nuclei (DAPI). I) 3-D renderings of calcified tissue in pellet and bead explants, and average volume of mineralized tissue in explants as assessed by μCT ($n = 5$).

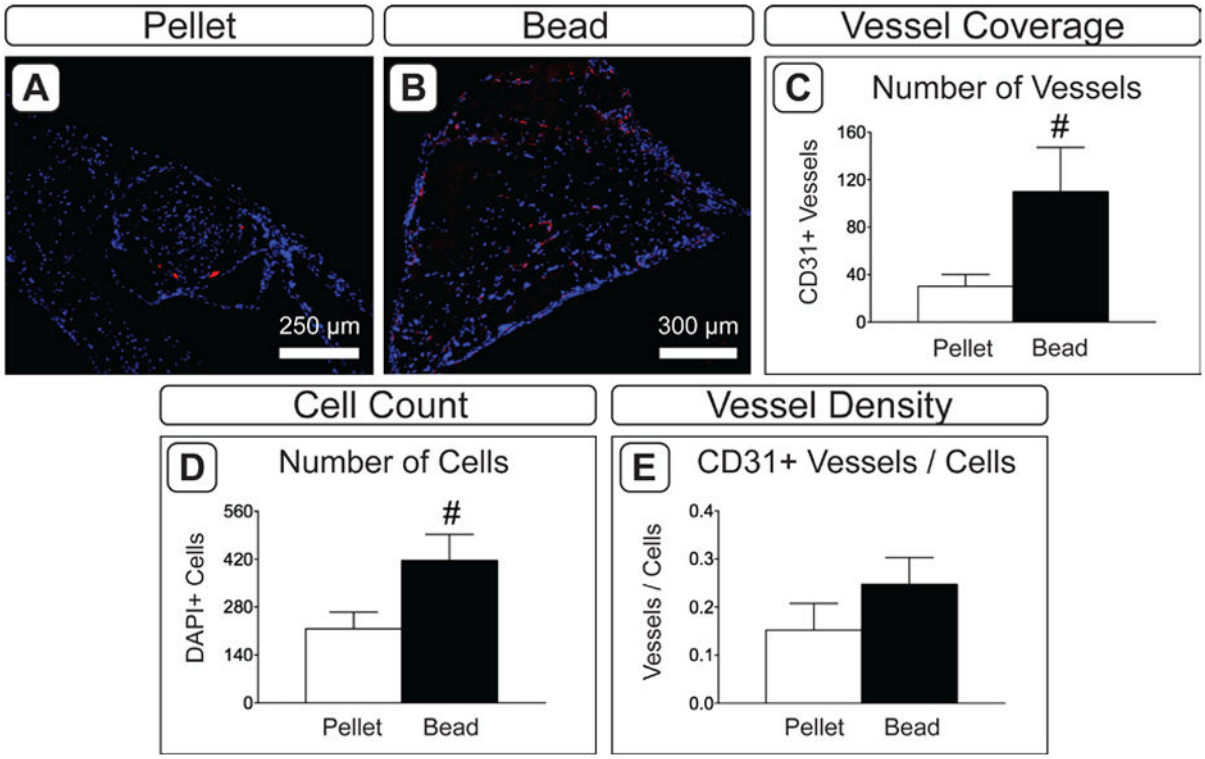


**Figure 5.**

Vascular invasion in 8 week explants. A,B) CD31 immuofluorescence in pellet (A) and bead (B) constructs. Red indicates positive staining; blue indicates cell nuclei (DAPI). C–F) Assessment of vascularization in explanted tissues. Blood vessel coverage was assessed by quantifying the number of CD31+ vessels (C) and the number of cell nuclei (D). A representative value for blood vessel density was calculated by normalizing to the number of vessels to the number of DAPI-positive cells (E). ($n = 6$; #: $p < 0.065$).

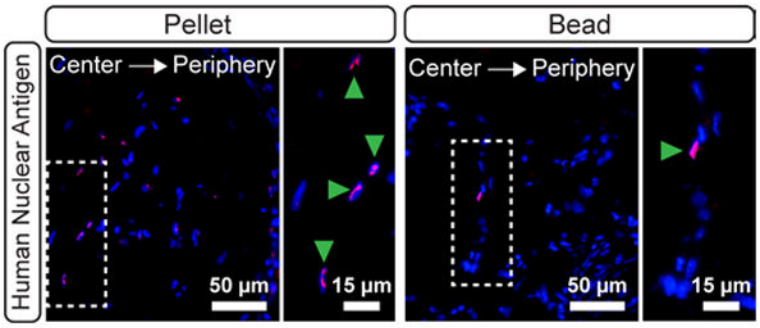


**Figure 6.**

Contribution of hASCs in 8 week explanted pellets (A) and beads (B). Magenta staining indicates positive staining for human nuclear antigen on hASCs. Blue indicates all cell nuclei (DAPI). The white dashed boxes indicate the locations of magnified areas in the right-hand panels. Green arrowheads denote human cells in the magnified regions.